BioGecko Vol 12 Issue 03 2023

ISSN NO: 2230-5807

Bleomycin carried on Fe_3O_4Nano-carrier effecting on BAX gene expression in Kidney cancer therapy

Samar Nahrawan[1], Salih Abdul-Mahdi[1], Sharafaldin Al-Musawi[2]
[1]Al-Qasim Green University,College of Biotechnology, , Babylon, Iraq
[2]Al-Qasim Green University,College of Food Sciences, , Babylon, Iraq

Abstract
Because distinctive super paramagnetic iron oxide nanoparticles (SPIONs) were used in antibacterial drugs and other biomedical applications.Here, a bleomycin (BLN)-delivering nanocarrier was made using a SPION wrapped with dextran (DEX) andgarnishedby folate (FA) to treat kidney cancer cells. Characteristics of prepared nanoparticles (NPs) were measured by using of typical procedures. In present study, the effect of that induced by SPION-DEX-BLN-FA was evaluated by using of methyl thiazolyl tetrazolium (MTT), and real time PCR (RT-PCR)techniqueon kidney cancer A-498 and healthy HK-2 cell lines was applied. The obtained results showed that prepared nanoparticles were smooth surfaces and spherical particles additional to good dispersity, and free from adhesion or accumulations with each other. The NPs sizes were 72.79 ± 23.95 nm, the polydispersity was 0.074, and the zeta value was -33.8 8.47 mV. As well as the in vitro results showed that FA-BLN-DEX-SPION revealed significant cellular cytotoxicity effects induction on A-498 kidney cell line. As well as it was found that the SPION-DEX-BLN-FA actually they are acted synergistically to target the delivery of bleomycin to A-498 kidney cancer cells. On the other hand the RT-PCR findings indicated that the level of mRNA BAX gene was higher expression 3.21fold upregulation when treated with SPION-DEX-BLN-FA compared with control (housekeeping gene). In conclusion the SPION-DEX-BLN-FA NPs it can be a promising therapeutic formulation for the treatment of kidney cancer in humans.
Keywords: Fe_3O_4, Nanoparticles, Bleomycin, BAX gene, , kidney cancer.

Introduction

As it is known that most of the standard cancer treatments are surgery, radiotherapy and chemotherapy, and this is applicable in all clinical practices. As the medicines for the treatment of cancer are given orally or intravenously, which reach to circulation and access those medicines to all body tissues whether it was targeted or not, which result in severe side effects such as immune depression or autoimmunity, some of which lead to damage to some non-targeted tissue (1,2)**.**

Here comes the role of nanoparticles in delivering insoluble drugs to remote target places in a safe manner and at a specific sites of the cell, thus minimizing the negative effects of the systemic use of traditional therapeutic drugs. Nanoparticles are small structures ranging in size from 1 to 100 nanometers. They exhibit significantly different physical and chemical properties than their larger counterparts (3).In general, nanoparticles cause death in cancer cells by producing reactive oxygen species, which is mediated by apoptotic or by protein production and reduction, immunological interferenceand cytotoxicity (4). Under oxidative stress, the up- and down-regulation of gene expression occurs when cells imitate a biological reaction to any endogenous or exogenous stimulus (5).BAX gene is the central cell death regulator, the Bax gene, is a crucial element. It is a crucial member of the LBL2 family that regulates apoptosis in both healthy and malignant cells. Any malfunction in the programmed cell death program make carcinoma cells resistant to treatment, and hence the cancerous tumors(6). Therefore, the study aimed to evaluate the role of super paramagnetic

iron oxide nanoparticle (SPION)nan-carrier that is composed of SPION coated with dextrin(DEX)and decorated with folate (FA) to encapsulate bleomycin (figure.1) for treating the kidney cancer cellthrough the carriedbleomycin drug on SPION-DEX-FA nanoparticles on the BAX gene expression, which is considered one of the genes that has a significant part in the activation of cell death, or programmed cell death

Figure. 1. Graphicalrepresentation of the production process for FA-BLM-SPION nanoparticles.

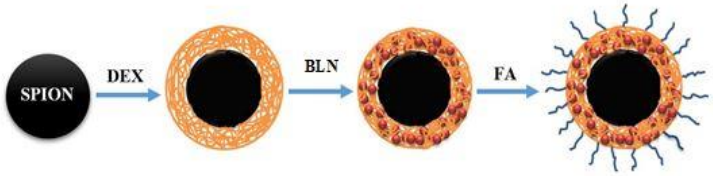

2. Materials and methods

2.1 Materials

The majority of the materials used in this investigation were approved by two businesses. The first was Merck, which provided the BLN medication, DEX, DMSO, FeCl36H2O, FeCl24H2O, MTT powder, NH4OH, and Folate, while ATTCC, USA provided the cancer A-498 and normal KH2 cell lines. The remaining supplies were bought from Sigma Aldrich in the USA.

2.2 SPION fabrication

Fe_3O_4 nanoparticles were prepared through co-precipitation procedure that is considered a common method to SPION preparation for biomedical application (7,8). Briefly preparation procedure involved the mixing of $FeCl_2.4H_2O$(99% 0.6gm) with $FeCl_3.6H_2O$ (99% 1.2 gm) then in 10 ml deionized water were dissolved. Finally the fabricated Fe_3O_4 nanoparticles were obtained after being dried in an oven at $65C^0$ for overnight.

2.3 SPION-DEX-BLM-FAformation

Albukaty 2020 and Levy in 2004 respectively were employed earlier techniques, by them the SPION-DEX-BLN-FA and using of the following mathematical question (1)was prepared (9,10). Then the final product was stored at $4C^0$ for potential uses.

$$\text{Encapsulation Efficiency (\%)} = \frac{\text{(Whole quantity of drug - Free quantity of drug)}}{\text{Overall amount of drug}} \times 100 \qquad \text{Eq.1}$$

2.4 Properties of synthesized nanoparticles

Morphological characteristics of prepared NPs were attained and recognized by several specialist devices; and it is as follows;high resolution transmission electron microscopy (HRTEM),field emission scanning electron microscopy (FESEM), fourier transform infrared spectroscopy (FTIR), X-Ray diffraction (XRD),dynamic light scattering (DLS), and vibrating sample magnetometer (VSM).

2.5Efficiency of drug encapsulation

The SPION-DEX-BLN-FA Nano-formulation was centrifuged for 30 minutes at 1500. The outcome was the precipitation of the nanoparticles. The free unloaded BLN medication will be suspended.The concentration of the BLN was determined using a425 nm-wavelength UV-Vis spectrophotometer following collecting all of the BLN in the supernatant. To ascertain whether medicine encapsulation was effective, the following equation (2) was used:

$$\text{Encapsulation Efficiency (\%)} = \frac{\text{(Total quantity of drug – Free quantity of drug)}}{\text{Total amount of drug}} \times 100 \qquad \text{Eq. (2)}$$

2.5 Drug release profile

One of the important steps in this work is to measure the amount and speed of drug release from the nanoparticle carrier. This step achieved by using of two types of buffers the first was phosphate buffer saline (FBS) with concentration is0.01 M, and pH 7.4 and the second buffer was citrate itsconcentration was0.01 M, pH=5.4 at 37C^0. Nonionic solution was added for both buffer solutions as an emulsifying factor to prevent the released medication from potentially sedimenting. Briefly 1ml of bleomycinladenBuffers were carefully agitated using a shaker while the experiment's temperature was set at 37C0 (GFL, Burgwedel, Germany).). The samplewas completedat period times as 0,4,8,12,14,24,48 and 72 hrs. Then drug release calculated by the following mathematical question (3)

$$R = \frac{V \sum_{i}^{n-i} C_i + V_o C_n}{m_{drug}} \qquad \text{Eq.2}$$

Where the letter R was representing of drug release (%), While V it is represented volume of sampling, $V_0$was representthe first dose of the medication, C_i as well as Cn weresymbolize to VLM concentration, whereas the symbols'i' and 'n'were are the sampling times. On the other hand 'mdrug' is the BLM drug that loaded on the FA-DEX-SPION carrier. All precipitated materials were rinsed and re-suspended in double distilled water (DDW).

2.6 Methyl thiazolyl tetrazolium (MTT) assay

Cytotoxicity effects on prepared nanoparticles was identified at different concentrations which was accomplished according to all the steps used in the study of Salim Al-bukhaty and his team (9). Briefly; 200µl of medium included 1 x10^4 cells in each well plate after 24 hours the old medium was replaced with a fresh medium involved (5 to 30µl) of either BLN, SPION-DEX-BLN-FAand FA-DEX-SPION thensubsequently incubation period for twenty four(24) and forty eight (48) hours. On the other hand non treated cells group were considered as a control. Subsequently MTT solution was added to each well then incubation at 37 C^0 with 95% air and 5% CO_2 for 4 hr. At the end the absorbance results of each samplewereWith a multi-scan plate reader, the data were captured at 540 nm.

.

2.7 Real Time-PCR assay

After 24 hours, treated cells were used to isolate ribonucleic acid (RNA) using (TRIzol ,UK). Then the isolated RNA converted to cDNA by synthesis Kit (Fermentas, Germany). For amplificationreverse and forward primer for β-Actin, and BAX genes (10,11,12) were utilized in this work .

$$\text{Relative cell toxicity} = [(^{A}\text{ sample} - ^{A}\text{ control})] \times 100 \qquad \text{Eq.4}$$

Table 1: The sequences of primers oligonucleotides used to amplify the studied genes.

Gene	Forward	Reverse
B-actin	5'-CTGGCACCCAGCACAATG-3'	5'-GCCGATCCACACGGAGTACT-3'
Akt1	5'- AGGTGACACTATAGAATA-3'	5'- GTACGACTCACTATAGGG-3'

Table 2. Time,Temperature and the number of cycles for each step.

Step	Temperature	Time	Cycles
Initial Denaturation	95 °C	10 min	1
Denaturation	95 °C	15 sec	45
Annealing	60 °C	1 min	
Melting curve analysis	95 °C	5 sec / step	1

3. Results

3.1 Morphological properties and size of synthesized NPs

Both Scanning and transition microscopes were used to determine the morphological properties and size of prepared Nano-particles. Images from both electron microscopes showed that every nanoparticle had a spherical shape, smooth surfaces, and acceptable dispersity (figure 2). Malven Zetassizer ZS, UK's DLS device was used to measure size and distribution, and the results revealed thatthe size and polydispersity of SPION were 29± 41 nm and -19.8 nm respectively (Figure 3 a &b). On the other hand figure 4a and b demonstrated the size and polydispersity of SPION-DEX-BLM-FA it was 72± 79 nm and 0.074 nm and -33.8 respectively.

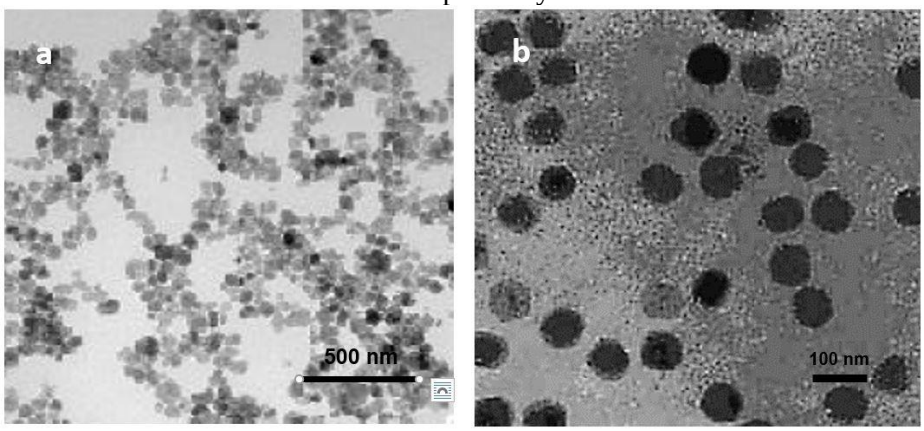

Figure 2. Morphological characteristics(a); HRTEM for SPION and (b); for SPION –DEX-BLN-FA nanoparticle

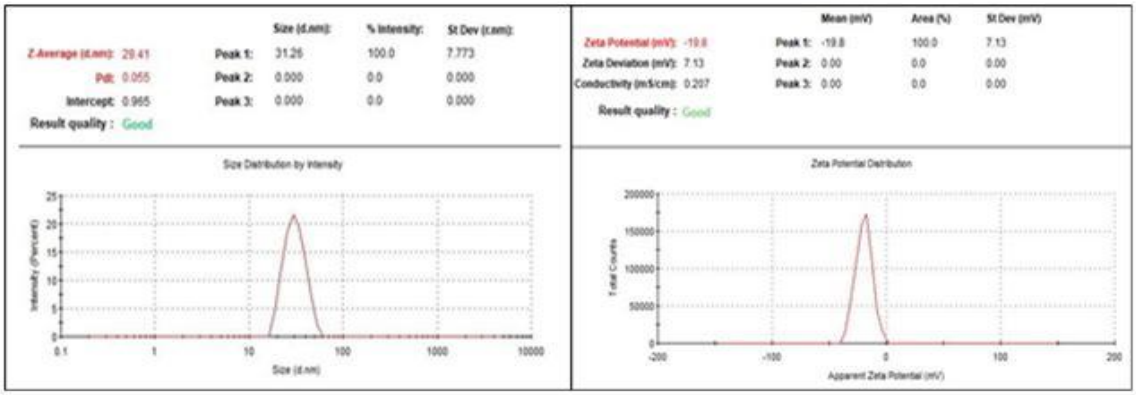

Figure 3. size (a) and charge (b) of SPION by DLS device.

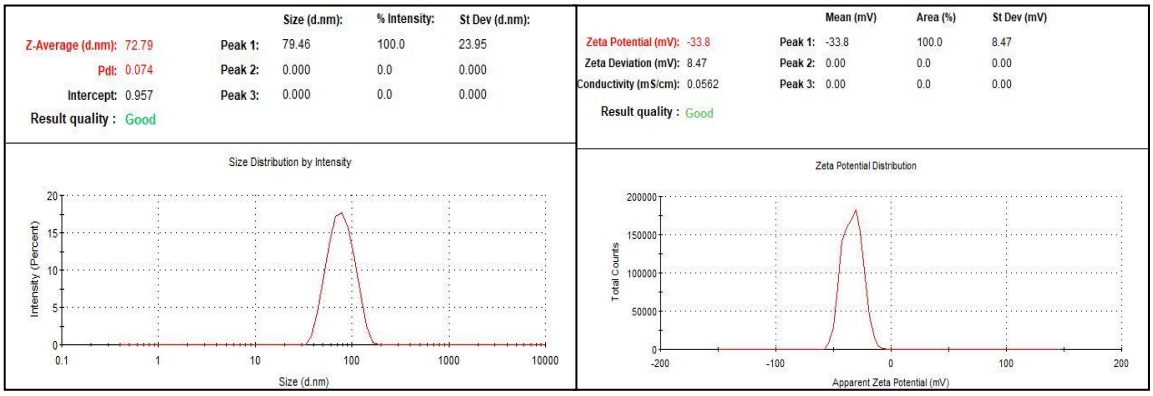

Figure 4. Size (a),charge (b) of SPION-DEX-BLN-FA using DLS device.

3.2 FTIR Fourier transform infrared spectroscopy

To confirm the functional groups on the surfaces of the nanoparticles manufactured in this study, Matson1000 FT-IR spectrophotometer (Unican, USA) and Potassium bromide pellet in the range of 4000 - 400 cm-1 region. were used.

The distinguished peaks of the polymer-encapsulated SPIONs were illustrated in (Figure.5). A major band at 591 cm1 was caused because of the vibration of Fe-O for all samples (13). the peak of absorption at3422 cm1 in the FT-IR spectra of naked SPIONs (Fig. 5a) demonstrates the presence of many hydroxyl groups on the surface of iron oxide particles were correlates to the stretching vibration of OH, which increases the tendency for agglomeration of the manufactured SPIONs(14).The peak at 1461 cm1 in the FT-IR spectrum of dextran-coated SPIONs is caused by the bending vibration of the C-H bond. The peak at 2919 cm1 is due to the stretching vibration of -CH2- groups. The vibrational motion of the etheric bond (C-O-), which is responsible for the absorption line at 1028 cm1, can be seen in Figure 5b.the distinctive peaks of BLN in SPION-DEX-BLN can be identified by comparing spectra b and c. In other words, it proved beyond a doubt that SPION-DEX and BLN were successfully captured.Due to SPION-DEX-functionalization BLN's with folate, the SPION-DEX-BLN-FA spectra had a peak at 1690 cm-1 that was associated with the carboxyl group of folic acid, confirming the existence of this molecule (15).

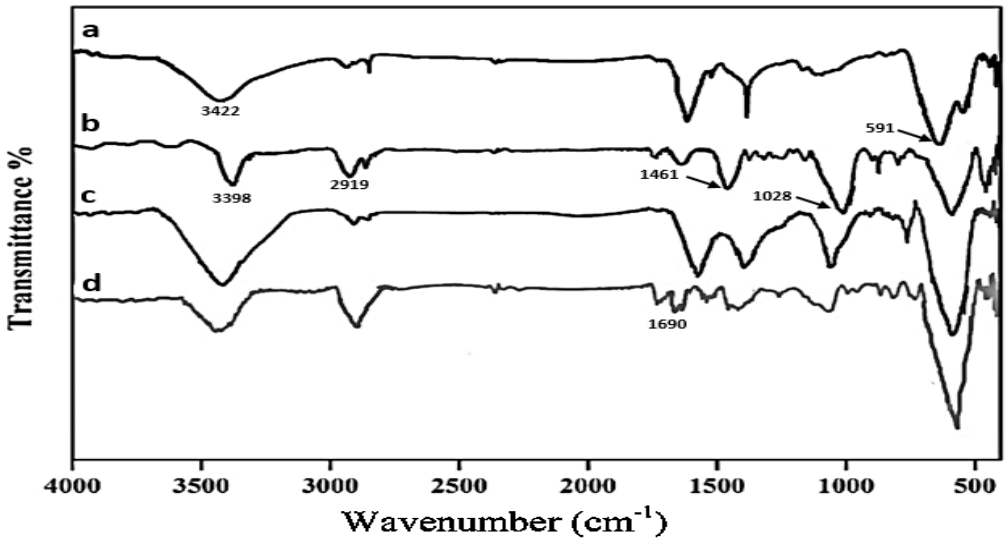

Figure. 5. FTIR spectra of (a, b, c, d)were for SPION, SPION-DEX, SPION-DEX-BLN (d)SPION-DEX-BLN-FA respectively.

3.3 VSM, (vibrating sample magnetometry)

Detection of magnetic characteristics of prepared nanoparticles, weredepicted in the SPION, Fe3O4-DEX, Fe3O4-DEX-BLN, and Fe3O4-DEX-BLN-FA in their natural forms. The findings demonstrated that the SPION without modification had a vibrating sample magnetometer of 61 emu/g, while the SPION-DEX had a vibrating sample magnetometer of 44 emu/g, in addition to thirty nine (39) and thirty (30) for the BLN loaded DEX,SPION and BLN loaded FA-DEX-SPION, respectively.This extraordinary inclusion of diamagnetic dextran in the Nano-formulation resulted in a decrease in saturation magnetization (16).

3.4 X-ray diffraction (XRD)

By observing the X-ray diffraction patterns, the crystalline characteristics of the fabricated NPs at each stage of manufacturing were examined. Patterns of X-ray diffraction respectively for each of the SPION, DEX-SPION, DEX-BLN-SPION and FA-BLN-DEX-SPION are depicted in Figure 6.Several peaks were also seen for naked SPION at 2 =17.95° (111), 29.80° (220), 36.03° (311), 44.10° (400), 54.21° (422), 56.93° (511) and 62.71° (440), which are classified as those of the inverted spinal structure of magnetite (JCPDS card No. 01-088-0866). (Figure. 6a). the peak intensities of the diffraction peaks were weakened and width was broadened (Figure6b and c). XRD resultswere also suggestive of nonappearance other forms of Fe3O4 in the manufactured product (17).On other hand the characteristic peaks of SPION-DEX and SPION-DEX-BLN, did not disappear and still be seen, however.While in the case of SPION-DEX-BLN-FAthe characteristic peaks almost disappeared may be due to polymer amorphous properties and bilayer coverage (Figure 6d).

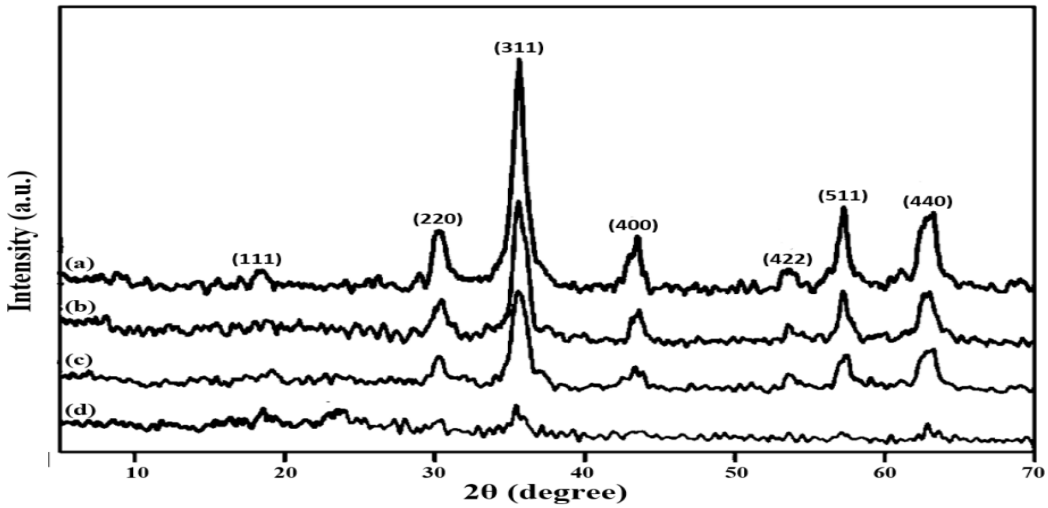

Figure 6. XRD spectra (a, b, c,and d) were for SPION ,SPION-DEX ,SPION-DEX-BLN,and SPION-DEX-BLN-FA

3.5 Drug encapsulation efficiency:

By the following question (2) the drug encapsulationefficacy was calculated. The encapsulation efficiency calculation came out to 83.2 3.4, indicating that the medicines were loaded properly onto DEX-SPION. At this point, the nanocomposite demonstrated great stability and suitable drug conservation.

$$\text{Encapsulation Efficiency (\%)} \quad \frac{\text{(Total quantity of drug – Free quantity of drug)}}{\text{Total amount of drug}} \times 100 \qquad \text{Eq. (2)}$$

$$\text{Encapsulation Efficiency (\%)} \quad \frac{\text{(1 mg – 0.17 mg)}}{\text{1mg}} \times 100 = 83\%$$

3.6 Methyl thiazolyl tetrazolium (MTT)

The FA-DEX-VBL-cytotoxicity SPION's results were tested using the MTT assay on the cancer cell line A-498 and the healthy cell line HK2.Cytotoxic effect after 48 hours of various concentrations (5–30 µg) of void BLN showed in (figure 11a)and the cytotoxicity effects of bare nanoparticles(SPION@DEX-FA) after 48 hoursin (figure.11b) while for SPION@DEX-BLN-FA in (figure.11c and d) for 24 and 48 hours respectively on A-498 kidney cancer and HK-2 normal cell lines.

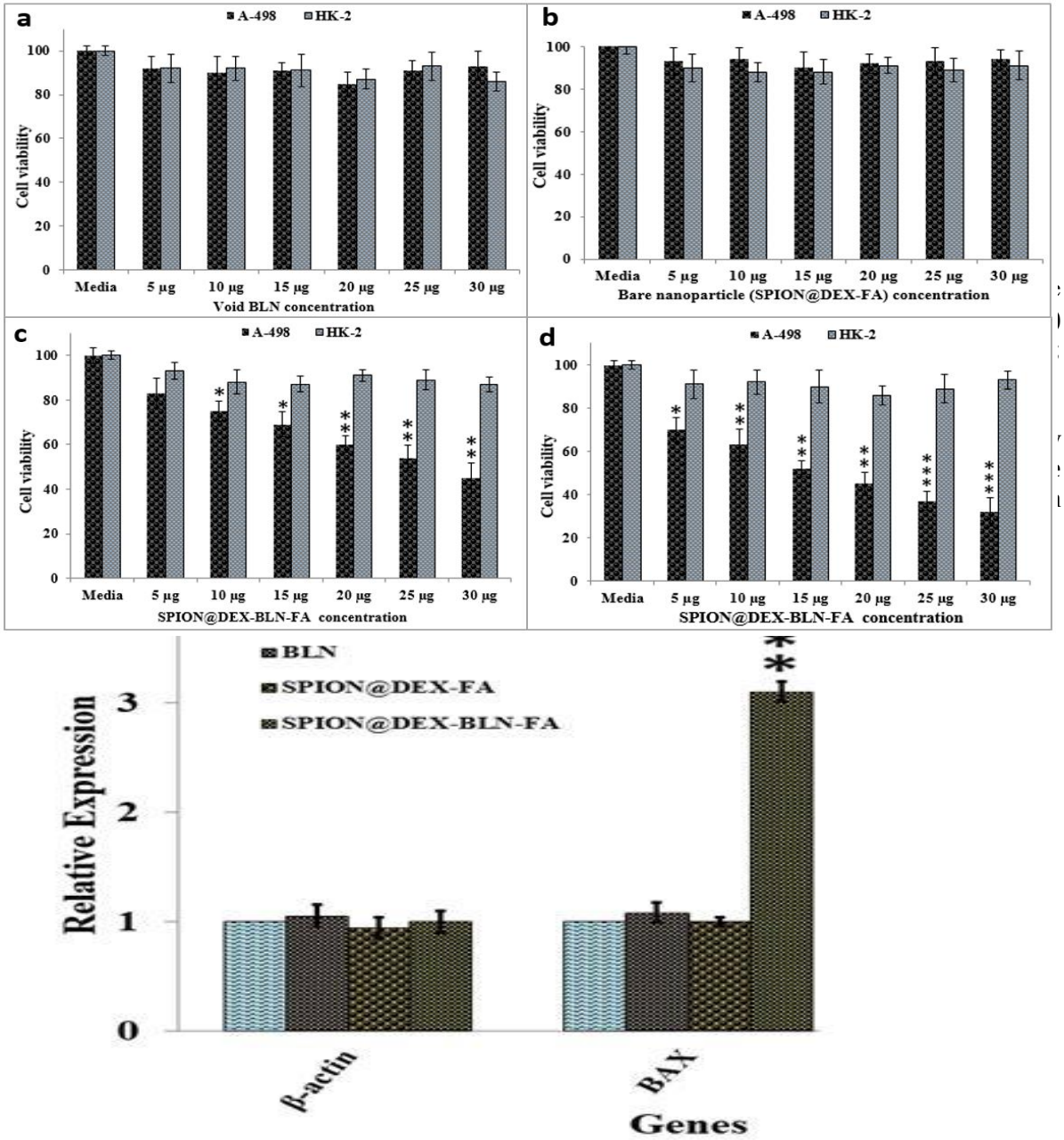

Figure 8.A real-time PCR gene expression analysis of A-498 cancer cells treated with void BLN, SPION-DEX-BLN-FA, and SPION-DEX-FA was utilized an ANOVA with a second-way analysis.The probability data were shown as the mean and standard deviation (SD) in the graph, which shows the differences between the control (untreated) and other treatments that are significant.

4.Discussion

The Fe_3O_4 NPs used in the current research were briefly made using a technique that involved mixing dissolved $FeCl_2.4H_2O$ and $FeCl_3.6H_2O$ in distal water with a few drops of ammonium hydroxide. The resulting precipitates contained Fe-NPs. TheFe_3O_4Nano-powder was successfully made using the chemical precipitation method, and our outcomes were consistent with the analysis of each and every one of them (18).Concerning functional groups on the surfaces of the nanoparticles manufactured in this study thedistinguished peaks of the bare and the coated SPIONs with polymer that were depicted in (Figure 5). A major band at 591 cm1 is due to the vibration of Fe-O for all samples (13) The FT-IR spectra of naked SPIONs show a peak absorption at 3422 cm1 (Fig. 5a).Iron oxide particle surfaces are found to have a significant number of hydroxyl groups, which is correspondto the stretching vibration of OH, which increases the proclivity for agglomeration of the manufactured SPIONs (14).

After creating the nanoparticles, the next step was to detect their properties, some of which include how quickly the medication bleomycin is released from the nanoparticle carrier (19). It was discovered that the rate at which BLN released from its Nano-carrierCompared to the phosphatase buffer's typical pH of 7.4, the acidic pH of the citrate buffer during 96 hours was greater (5.4).The suitable interpretation for such result may correspond with Hecht in 2000 it was reported that the solubility of bleomycin in acidic more than in alkaline buffers, it was 13.0 mg/ml and 10mg/ml respectively (20).

With regard to cytotoxicity of bleomycin medication on Kidney A-498 cancer and HK2 heath cell lines the present findings revealed that the high concentration (25,30 g) of SPION-DEX-FA demonstrated significantly ($p<0.001$) decreased cell growth of Kidney A-498 cancer (**$p < 0.01$; *** $p < 0.001$)for 24 and 48 hours respectively compared with HK2 control cell lines .

RT-PCR results revealed that level of BAX expression was 3.21fold up regulation show significantly difference $p <0.001$when treated with DEX-SPION-BLN-FA compared with control (housekeeping gene).Sample indicated its inhibitory capabilities on the growth and proliferation of cell tumors cells. That indicates that the medicine was successfully carried by its nanoparticle carrier to targeted cancerous cells, where it then targeted the BAX gene and gave more proof that human kidney cancer underwent to apoptosis (21,22).According to several studies, the Bcell lymphoma-2 homology 3 (BH3) domain of the direct activator BH3-only proteins, such as tBID and BIM, interacts with BAX upon the activation of apoptosis to cause BAX accumulation at specific puncta at the mitochondrial outer membrane (MOM) known as apoptotic foci. (23,24). However, the mechanism by which the bleomycin affected the BAX gene expression remains uncertain.These findingssimilartoAl-Musawi result in 2020 had been reported that the expression of BAXgenewas increased in breast cancer treated with the SPION-Au-CS-DOX-FA compared SPION-AU-DEX-FA.As a result, developed SPION-DEX-BLN-FA may be an advantageous therapeutic formulation for the treatment of clinical kidney cancer.

References

1. Deepa Mundekkad1 and William C. Cho2. Nanoparticles in Clinical Translation for Cancer Therapy. Int J Mol Sci. 2022; 23(3): 1685.
2. Wang J., Li Y., Nie G. Multifunctional biomolecule nanostructures for cancer therapy. Nat. Rev. Mater. 2021;6:766–783.
3. Sweeney E.E., Balakrishnan P.B., Powell A.B., Bowen A., Sarabia I., Burga R.A., Jones R.B., Bosque A., Cruz C.R.Y., Fernandes R. PLGA nanodepots co-encapsulating prostratin and anti-CD25 enhance primary natural killer cell antiviral and antitumor function. Nano Res. 2020;13:736–744.

4. Kim U., Kim C.-Y., Lee J.M., Oh H., Ryu B., Kim J., Park J.-H. Phloretin inhibits the human prostate cancer cells through the generation of reactive oxygen species. *Pathol. Oncol. Res.* 2020;26:977–984.
5. Grueso M.J.L., Valero R.M.T., Carmona H.B., Ruiz D.J.L., Peinado J., McDonagh B., Aguilar R.R., Ruiz J.A.B., Peña C.A.P. Peroxiredoxin 6 down-regulation induces metabolic remodeling and cell cycle arrest in HepG2 cells. Antioxidants. 2019;8:505.
6. Zhiqing Liu, Ye Ding, Na Ye, Christopher Wild, Haiying Chen, Jia Zhou. Direct Activation of Bax Protein for Cancer Therapy. Med Res Rev. 2016;36(2):313-41
7. M., Koutsopoulos A. V., Darivianaki K., Delides G., Siafakas N. M. and Bouros D. (2005). Expression of apoptotic and antiapoptotic markers in epithelial cells in idiopathic pulmonary fibrosis. *Chest* 127, 266-274. 10.1378/chest.127.1.266.
8. Al-Musawi, S.; Kadhim, M.J.; Hindi, N.K.K. Folated-nanocarrier for paclitaxel drug delivery in leukemia cancer therapy. J. Pharm. Sci. Res. 2018, 10, 749–754.
9. Albukhaty, Sharafaldin Al-Musawi, Salih Abdul Mahdi, Ghassan M. Sulaiman ,Mona S. Alwahibi, Yaser Hassan Dewir, Dina A. Soliman, and Humaira Rizwana. Investigation of Dextran-Coated Superparamagnetic Nanoparticles for Targeted Vinblastine Controlled Release, Delivery, Apoptosis Induction, and Gen Expression in Pancreatic Cancer Cells. Molecules 2020, 25, 4721.
10. SLévy R, Thanh NTK, Doty RC, et al. Rational and combinatorial design of peptide capping ligands for gold nanoparticles. J Am Chem Soc. 2004;126(32):10076–10084.
11. Abdul Mahdi S, Kadhim AA, Albukhaty S, Nikzad S, Haider AJ, Ibraheem S, Kadhim HA, Al-Musawi S. Gene expression and apoptosis response in hepatocellular carcinoma cells induced by biocompatible polymer / magnetic nanoparticles containing 5-Fluorouracil. Electron J Biotechnol. 2021; 52, 21–28.
12. Al-Musawi, S.; Albukhaty, S.; Al-Karagoly, H.; Almalki, F. Design, and Synthesis of Multi-Functional Superparamagnetic Core-Gold Shell Coated with Chitosan and Folate Nanoparticles for Targeted Antitumor Therapy. Nanomaterials 11(1):32.
13. Al-Musawi, S.; Ibraheem, S.; Mahdi, S.A.; Albukhaty, S.; Haider, A.J.; Kadhim, A.A.; Kadhim, K.A.; Kadhim, H.A.; Al-Karagoly, H. Smart Nanoformulation Based on Polymeric Magnetic Nanoparticles and Vincristine Drug: A Novel Therapy for Apoptotic Gene Expression in Tumor. Life. 2021; 11, 71.
14. Ahmad S, Riaz U, Kaushik A. Soft template synthesis of super paramagnetic Fe3O4 nanoparticles a novel technique. J Inorg Organomet Polymer Mater. 2009;19:355–60.
15. Sadighian S, Rostamizadeh K, Hosseini-Monfareda H, Hamidi M. Doxorubicin-conjugated core–shell magnetite nanoparticles as dual- targeting carriers for anticancer drug delivery. Colloids Surf B Biointerfaces. 2014;117:406–13.
16. Bai H, Liu Z, Delai SD. Highly water soluble and recovered dextran coated Fe3O4 magnetic nanoparticles for brackish water desalination. Sep Purif Technol. 2011;81:392–9.
17. Petcharoen K, Sirivat A. Synthesis and characterization of magnetite nanoparticles via the chemical co-precipitation method. Mater Sci Eng B. 2012;177:421–7.
18. Zhu, Y.; Yang, L.; Huang, D.; Zhu, Q. Molecularly imprinted nanoparticles and their releasing properties, bio-distribution as drug carriers. Asian J. Pharm. Sci. 2017, 12, 172–178.
19. Li, J., Ding, Y., Cheng, Q., Gao, C., Wei, J., Wang, Z., ... & Wang, R. (2022). Supramolecular erythrocytes-hitchhiking drug delivery system for specific therapy of acute pneumonia. Journal of Controlled Release, 350, 777-786.

20. Osial M, Rybicka P, Pękała M, Cichowicz G, Cyrański MK, Krysiński P.(2023) Easy Synthesis and Characterization of Holmium-Doped SPIONs. Nanomaterials (Basel). 13;8(6):430.
21. Ghasemi, A., Khanzadeh, T., Heydarabad, M. Z., Khorrami, A., Esfahlan, A. J., Ghavipanjeh, S., ... & Azimi, A. (2020). Evaluation of BAX and BCL-2 gene expression and apoptosis induction in acute lymphoblastic leukemia cell line CCRF-CEM after high-dose prednisolone treatment. Asian Pacific journal of cancer prevention: APJCP, 19(8), 2319.
22. Hecht,S.M. Bleomycin; New perspective on the mechanism of action. J.Nat.Prod. 2000; 63,158-168.
23. Dana Westphal, Grant Dewson, Peter E. Czabotar, Ruth M. Kluck. Molecular biology of Bax and Bak activation and action. Molecular Cell Research.2011; 4, 521-531.
24. Andreas Jenner, Aida Peña-Blanco, Raquel Salvador-Gallego, Begoña Ugarte-Uribe, Cristiana Zollo, Tariq Ganief, Jan Bierlmeier, Markus Mund, Jason E Lee, Jonas Ries, Dirk Schwarzer, Boris Macek, and Ana J Garcia-Saezcorresponding author. DRP1 interacts directly with BAX to induce its activation and apoptosis. EMBO J. 2022 Apr; 41(8).